# Establishing of soil loss tolerance limit and sediment yield in Zagros fold-thrust belt: a case study in the Kanarwe river basin, Iraq-Iran

Fahmy O. MOHAMMED[a], Ahmed I. MOHAMED[b]*, Ibrahim H. GART[c], Diary A AMIN[d]

[a]*Department of Earth Sciences and Petroleum, University of Sulaimani, Sulaymaniyah, Iraq.* 0000-0003-3755-0949
[b]*Department of English, Basic Education College, Tikrit University, Tikrit, Iraq.* 0000-0001-9226-0982
[c]*Ministry of Education, General Directorate of Education of Kirkuk, Kirkuk, Iraq.* 0009-0009-8257-1328
[d]*Sulaimani Polytechnic University, Sulaymaniyah, Iraq.* 0000-0001-6630-1226

[*]*Corresponding author*: *Ahmed MOHAMED*, *ahmed.moh@tu.edu.iq*

**ABSTRACT**
Soil degradation is a significant cause of topsoil loss; in most mountainous region watersheds, it leads to decreased agriculture productivity and reservoir storage. This study targeted calculating and mapping soil loss and sediment yield in the Lesser Zab watershed located between Iraq and Iran. The Revised Universal Soil Loss Equation (RUSLE) model was used to calculate the soil loss. A Digital Elevation Model of 30m, a Digital Soil map (1:500000), rainfall, and land cover were used to derive parameters. The soil loss rates are 58.1 and 0.1 t $ha^{-1}yr^{-1}$. The total annual soil loss is 1037289 tonnes, of these 404512, covering 75% of Kanarwe river basin land. Most of these affected lands are in the eastern and middle part, which is below the FAOs standard allowable for tolerable soil erosion. Still, the rest covers 25 % of the basin in the west with a total annual soil loss equal to 632777 tonnes, above FAOs standard. The maximum and minimum sediment yield is 29 and 0.1 $tha^{-1}yr^{-1}$, respectively. Based on the statistical correlation coefficient, the most effective RUSLE *Ahmed MOHAMED* parameters on sediment yield from high to low are topography 0.48, soil erodibility 0.38, and crop management 0.38.

Keywords: RUSLE, Sediment Delivery, Zagros Thrust Zone, CN-SCS Curve, Dam Lifespan

## 1. Introduction

Soil erosion is a geomorphic process that occurs naturally; however, humans' soil utilization and climate change lead to increased land degradation (Pennock, 2019; Yang et al., 2003). Soil loss particles are turned into sediments and delivered to the river by an erosion agent (Chuenchum et al., 2020), and erosion processes pose severe threats to agricultural production, dam lifespan, and the earth's landform (Balabathina et al., 2020; Lee et al., 2014). Man-made activities cause ten times faster soil loss than natural agents such as rainfall or coastal waves (Pimentel and Burgess, 2013). Sometimes, trapped sediment yield by a natural or artificial agent leads to bank erosion and decreased riparian vegetation (Anthony et al., 2015).

The RUSLE equations were first developed on a small scale in the United States of America but later were used and calibrated in many countries (Alewell et al., 2019; Ezzaouini et al., 2020). New studies suggest that integrating the Revised Universal Soil Loss Equation (RUSLE) with satellite image data is more effective for calculating amounts of soil loss and mapping its distribution(Kebede et al., 2021; Somasiri et al., 2021).

The soil loss and sediment yield recently threatened water quality and quantities in Iraq and Iran due to poor management of soil loss (Zare et al., 2017; Band et al., 2022; Ostovari et al., 2022; Othman et al., 2022; Salar, 2022). The unmanaged soil loss from the upstream country (Iran) and downstream sediment delivery decreased

dams' storage capacity and water resource life structures in the lesser Zab watershed within Iraq (Bhattarai and Dutta, 2007; Omeed H. Al-Kakey et al., 2022).

Many studies try calculating Iraq's sediment yield and soil loss, but the results are inaccurate. Hassan et al. (2016) studied sediment deposited types with the Dokan dam reservoir (DDR), located downstream of the Lesser Zab watershed, without considering the amount of Soil erosion risk and its effect on ecosystem management. Ezz-Aldeen et al. (2018) studied watershed sediment of DDR using the soil and water assessment model (SWAT) to estimate sediment delivery ratio-based Empirical Equation (Lumped model). However, this model is only applicable to small watersheds, not a watershed like DDR. Othman et al. (2022) conclude that the sediment yield is more than the soil loss, which is scientifically wrong. The soil erosion risk in Iran is also the same as in Iraq and many studies conclude that the risk of soil erosion has increased in the last decade (Sadeghi, 2017; Zare et al., 2017; Hosseinalizadeh et al., 2020).

Therefore, this study aims to answer four key research issues; How much soil eroded annually from the Lesser Zab watershed located between Iraq and Iran? Are the soil erosion processes uniformly over the basin or abnormally distributed over the Lesser Zab watershed? Is the potential for soil loss greater than the FAO's soil erosion tolerance limit? Which parameters of RUSLE are more significant on soil loss? This study's findings will serve as a benchmark for future dam site selection and ecosystem management in Iraq.

## 2. Research Methods

### 2.1 Study area and Data source

The Kanarwe River basin is part of the lesser Zab transboundary watershed within the Zagros Mountain Range (Figure 1). The basin outlet is 20 km away from northeast Sulaymaniyah city with a catchment area of 1541 $km^2$ and extended about 71 km in length (Mohammad, 2023). The Mediterranean climate's hot summers and wet winters deliver more than 800 mm of rain and have an average temperature of 20°C per year (Abbas et al., 2017; Shubbar et al., 2017; Mohammed et al., 2021;). Several data sources to estimate soil erosion based on the RUSLE. Field survey and ground truth collection by a Global Position System (GPS) include soil sampling and lithology description. A (30*30 m) DEM from the Advanced Spaceborne Thermal Emission and Reflection Radiometer (ASTER; GDEM) dataset is used to derive slope length- steepness factor value. The geological map of study area (Figure 2 a) was correlated with soil maps to measure accuare soil depth about geological units (Al-Qayim et al., 2018; Ma'ala, 2007). Soil map derived from the Harmonized Soil World Database (HWSD) (Figure 2 b)., with a scale of 1:500000 (Buringh, 1960; Nachtergaele et al., 2008) Mean annual rainfall data (1990–2015) from the four-

gauge stations (Dokan, Chwarta, Mawat, and Penjween) obtained from Sulaymaniyah metrological Directorate was used to estimate the annual mean rainfall at Kanarwe river basin (Mohammed et al., 2023) (Figure 3).

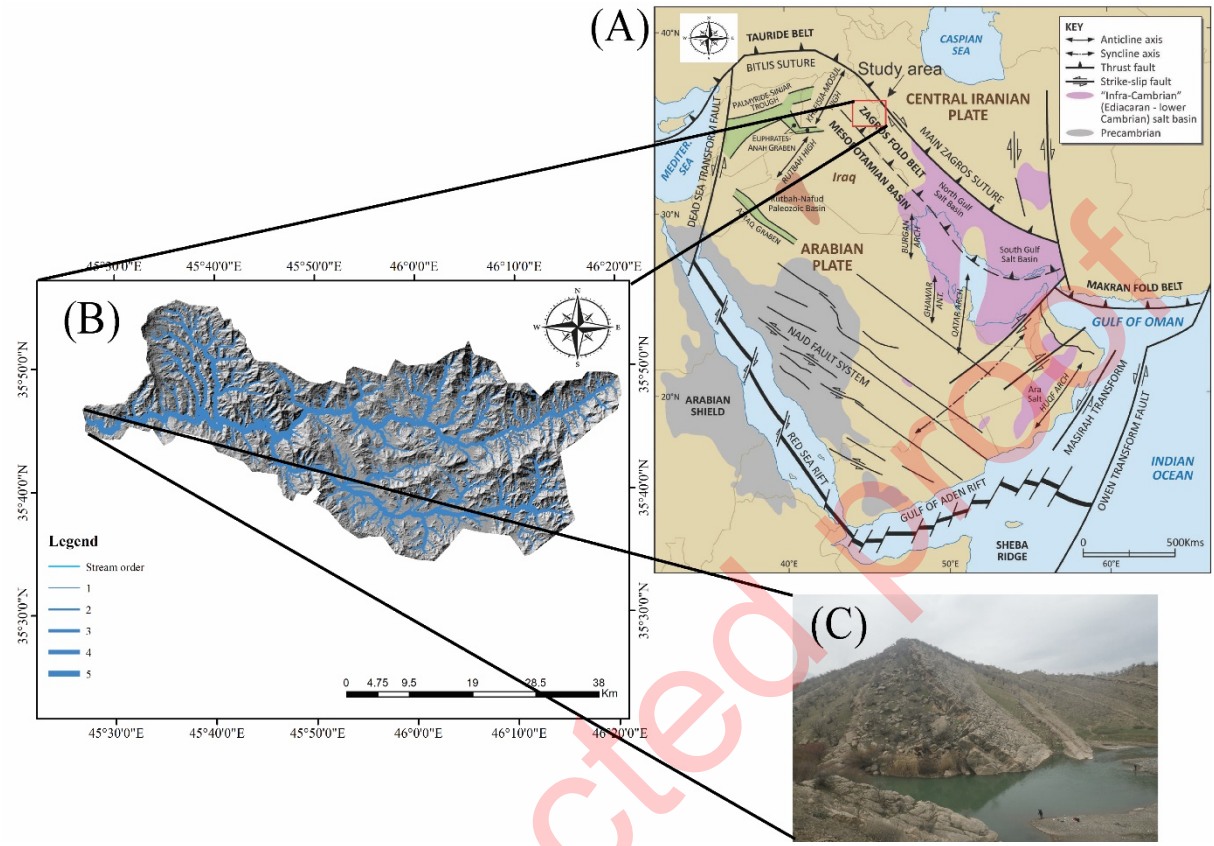


Figure 1- a) Regional tectonic setting Zagros mountains (English et al., 2015), b) Stream network of Siwail River that flows toward basin outlet (Dam site, East west), c) Proposed dam site.

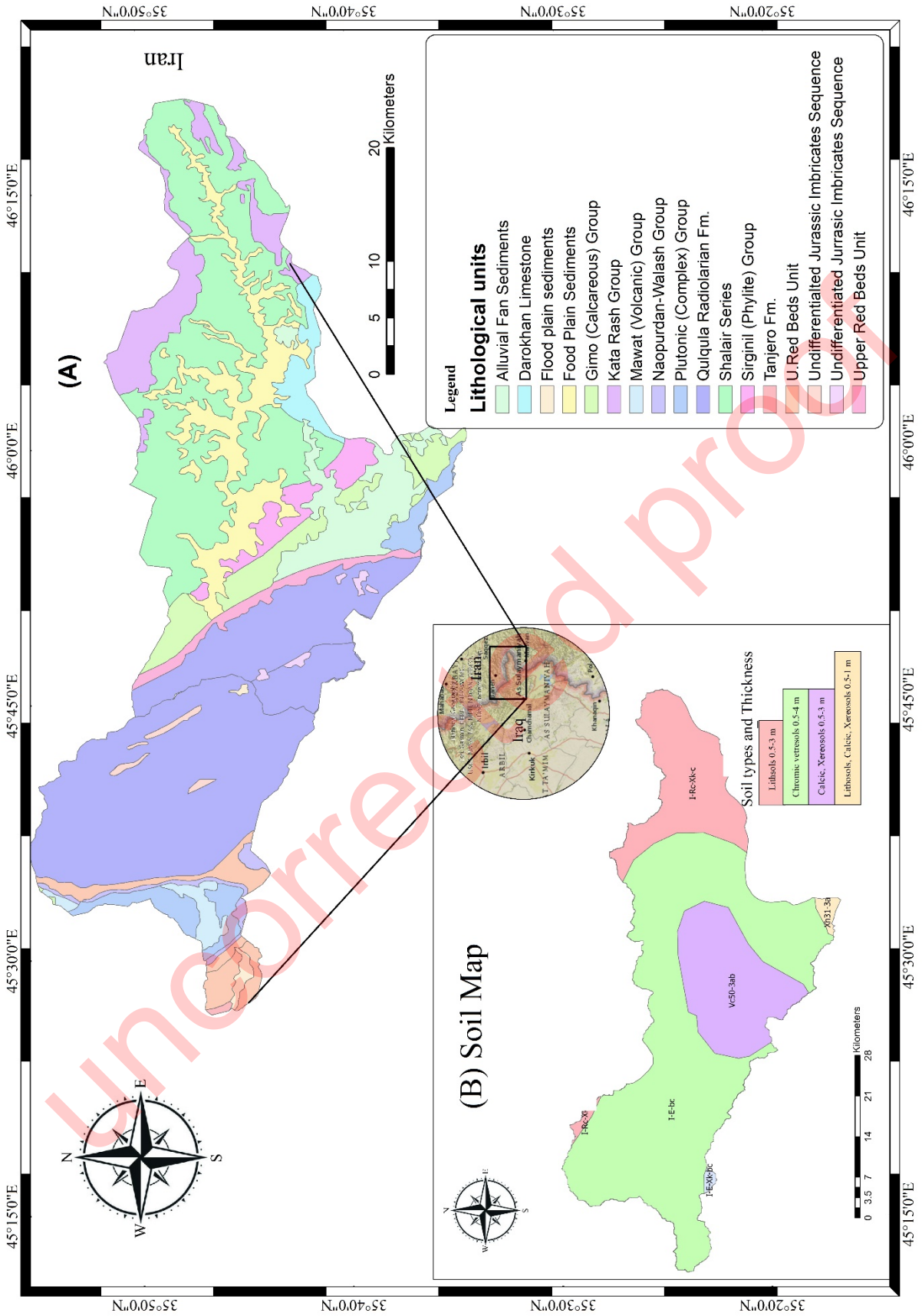


Figure 2- a) Show the geological map after ( Ma'ala, 2007; Al-Qayim et al., 2018), b) Soil map of the study area after (Buringh, 1960).

The Global Land Use and Landcover (LULC) map was obtained from the Global Land Cover Facility (www.landinfo.com) for determining soil erodibility, cover management, and SCS-CN number.


Figure 3- Mean monthly rainfall (blue bars) and temperature (red line).

## 3. Data Analysis

### 3.1 Soil loss estimation and Sediment yield

The soil loss was calculated using the RUSLE, an empirical model developed by Renard in (1997) to estimate soil loss. The RUSLE model Equation 1 is expressed as:

$$S_{loss} = R_E * Ks * LS_T * C_V * P_E \quad (1)$$

Where $S_{loss}$ is the mean annual soil loss due to water erosion (in tons per hectare per year (t $ha^{-1}$ $year^{-1}$)), $R_E$ is the rainfall and runoff erosivity factor (in MJ-mm $ha^{-1}$ $h^{-1}$ $year^{-1}$ ), Ks is the soil erodibility factor (in tone $ha^{-1}$ $MJ^{-1}$ $mm^{-1}$); L is the slope length factor (dimensionless), S is the slope steepness factor (dimensionless); C is the cover and management practice factor (dimensionless), and $P_E$ is the erosion support practice (dimensionless). The sediment delivery ratio (SDR; t.$ha^{-1}$ $yr^{-1}$) was calculated based on Equation 2.

$$SDR = 1.366 \times 10^{-11} *(DA) -0.0998 *(RL) 0.3629 *(SCS\text{-}CN) 5.444 \quad (2)$$

Where DA is the drainage area in $km^2$, RL is a relief-length ratio in m $km^{-1}$, and SCS-CN is the soil conservation service curve number. Finally, the sediment delivery ratio was used with Soil loss rate Equation 3 to calculate the sediment yield (Sy; t. $ha^{-1}$ $yr^{-1}$).

$$Sy=SDR*Ri \quad (3)$$

Where Ri is soil erosion for each grid cell.

Spatial analysis techniques and satellite images were used to simulate the RUSLE model, sediment delivery ratio, and sediment production., as shown in Figure 4.

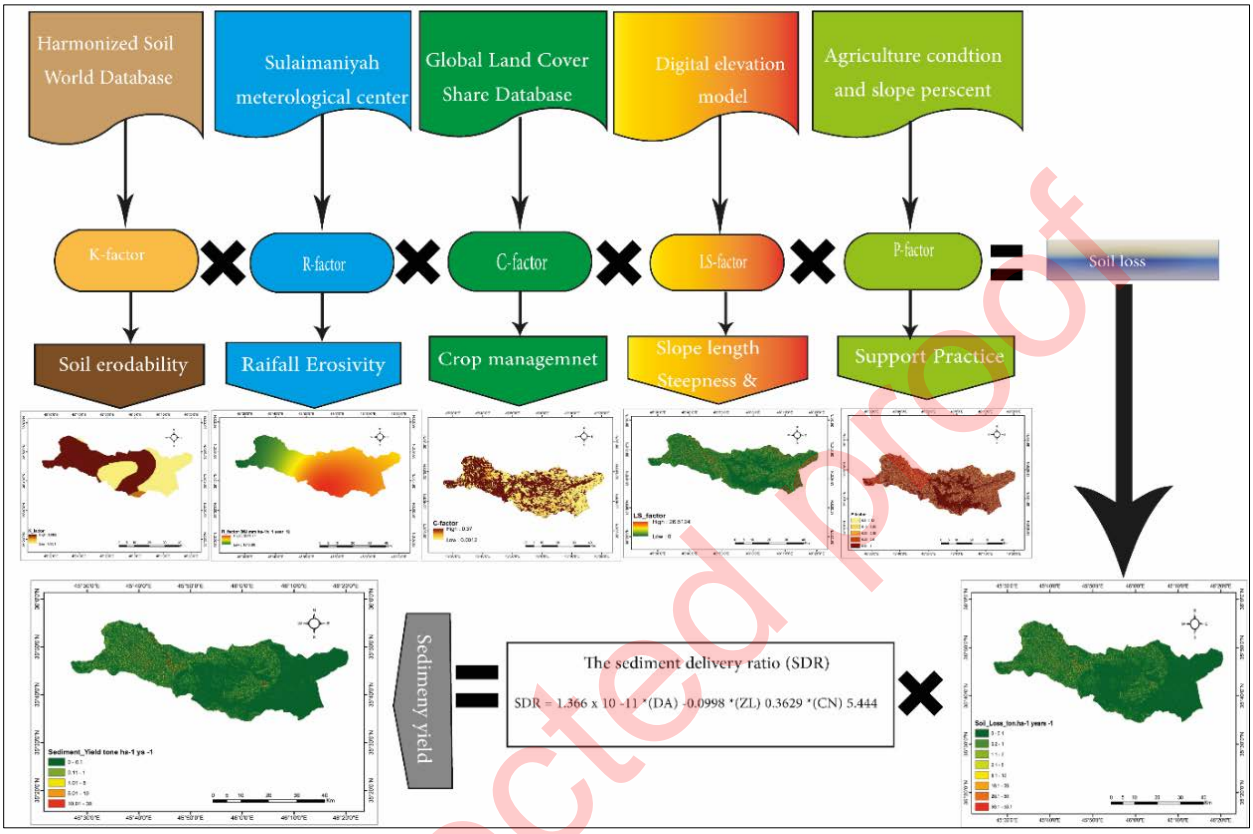


Figure 4- Conceptual modelling of estimation of RUSLE parameters.

### 3.2 Rainfall erosivity ($R_E$)

Rainfall erosivity is the erosive power of participation kinetic energy: the greater the intensity and rainstorm duration, the higher the erosion potential (Gholami et al., 2021). The $R_E$ factor is generally calculated from mean annual rainfall data using storm energy over a 30-min duration expressed by R = EI30 Equation 4.

$$R = \frac{1}{n}\sum_{j=1}^{n}\left[\sum_{k=1}^{m}(E)(I_{30})k\right]_j \quad (4)$$

where n is the total number of years where data was collected, K is the total number of rainfall storms up to m, j is several years up to n, $I_{30}$ is the maximum 30 min intensity (mm $hr^{-1}$), Ej is the total kinetic energy (MJ $ha^{-1}$) of a k storm in *m* year. (Renard and Freimund, 1994) Developed (Equation 5).

$$R_E = 0.04830*P1.61 \qquad P \text{ is less than } 850\text{mm} \quad (5)$$

where R = Rainfall Erosivity, P = Mean annual rainfall in mm.

For calculation ($R_E$), four stations' long-term mean annual rainfall (1990 to 2015) was obtained from the Sulaymaniyah Meteorological Directorate Table 1. For creating an erosivity map, the inverse distance weighted (IDW) approach is used to estimate the unknown cell value of erosivity for the whole watershed.

Table 1- Rain gauge stations, source (Sulaymaniyah Directorate of Meteorology and Seismology)

| No. | Gauging station | Location | | Altitude(m) | Mean annual rainfall |
|---|---|---|---|---|---|
| | | Longitude | Latitude | | |
| 1 | Penjween | 45.945478 | 35.627854 | 1280 | 950 |
| 2 | Chwarta-Mawat | 45.409533 | 35.902678 | 1160 | 700 |
| 3 | Dokan | 44.958625 | 35.952052 | 540 | 640 |
| 4 | Sulaymaniyah | 45.435350 | 35.566579 | 880 | 650 |

### 3.3 Soil erodibility ($K_S$)

The soil erodibility factor ($K_S$) assesses how vulnerable soil types are to particles being separated and carried away by rainfall and runoff. (Wischmeier and Smith, 1978). The soil types in the study area are classified into four classes-based FAO soil maps. The $K_S$ value for each soil class is calculated based on soil types, composition, and texture Table 2.

Table 2- KS value for Soil types based on (Buringh, 1960).

| Soil classification | Soil Texture | Ks |
|---|---|---|
| Lithosols | Clay and Loam. | 0.001 |
| Chromic vertosols | Loam to clay with variable gravel | 0.065 |
| Calcic xerosols | Clay marl gravel | 0.065 |
| Lithosols, Calcic, xerosols | Silty clay gravel | 0.0041 |

### 3.4 Topography ($LS_T$)

The topographic factors, such as slope length (L), represent the length between the starting and end of the inter-rill erosion process, and slope steepness (S) depends on steepness only. The LS factor is crucial in water movement (volume and velocity) in streams, considerably inducing soil erosion and Sediment transporting capacity (Gashaw et al., 2017). The LS factor in the RUSLE was estimated using spatial analysis techniques based on Equation 6 and Equation 7 (Simms et al., 2003).

$$LST = [A/22.13]^{0.6} * [sinB/0.0869]^{1.3} \quad (6)$$

where A is the upslope contributing area factor, and B is the slope angle. Incorporating the DEM into GIS accurately determined the slope gradient S and length L. This study computed the $LS_T$-value based on a modified Equation 7 suggested by ( Simms et al., 2003; Gelagay and Minale, 2016; Chuenchum et al., 2020) because upslope contributing and basin geometry is more influenced than slope length and steepness topsoil loss.

$$LS_T = \text{Pow}\left(\frac{\text{Flow accumulation} * (\text{DEM resolution})}{22.13}\right)^{0.6} * \text{Pow}\left(\frac{\sin(DEM\ slope) * 0.01745}{0.0869}\right)^{1.3} \quad (7)$$

Where Pow (power) is a function in the ArcGIS Spatial Analyst (Ashiagbor et al. 2013), the flow accumulation number of cells contributes to downward flow.

### 3.5 Cropping types($C_V$)

The cover management factor is the soil loss ratio soil loss rate and land cover types (Wischmeier and Smith 1978). Benavidez et al. (2018) prefer using previous research papers on land use/land cover to estimate the $C_V$ factor. This strategy was performed for the estimation $C_V$ factor Table 3.

Table 3- $C_V$ Factor Values for LUC types

| **Land cove** | **C** | **Source** |
|---|---|---|
| Rainfed croplands | 0.07 | (Yang et al., 2003) |
| Mosaic cropland | 0.37 | (Tiwary et al., 2014) |
| Mosaic vegetation | 0.25 | (Yang et al., 2003) |
| Closed (>40%) needle-leaved evergreen | 0.0015 | (Chadli, 2016) |
| Closed to open (>15%) mixed broadleaved and needle | 0.1 | (Chen et al., 2019) |
| Mosaic forest or shrubland | 0.01 | (Tiwary et al., 2014) |
| Mosaic grassland | 0.2 | (Tiwary et al., 2014) |
| Closed to open (>15%) (broadleaved or needle-leaved, evergreen, or deciduous) | 0.0012 | (Chadli, 2016) |
| Sparse (<15%) vegetation | 0.01 | (Yang et al., 2003) |
| Bare areas | 0.35 | (Yang et al., 2003) |

### 3.6 Support soil resistance method ($P_S$)

$P_S$ values range from zero to one, with zero indicating an ideal human-made structure for preventing erosion and one indicating no erosion resistance (Renard and Freimund, 1994). Such resistance structures include contour plowing, strip cropping, and terracing, controlled slope. (Shin, 1999) assigned $P_S$-value for five slope percentage categories based on slope percentage Table 4.

Table 4- The P factor value (Shin, 1999).

| Slope (%) | Land use | P factor |
|---|---|---|
| 9–12 | Non-Agriculture | 0.6 |
| 13–16 | Non-Agriculture | 0.7 |
| 17–20 | Non-Agriculture | 0.8 |
| 21–25 | Non-Agriculture | 0.9 |
| >25 | Non-Agriculture | 0.95 |

## 4. Results and Discussion

Three different software, including ArcGIS, WMS11.1 (watershed modelling surface), and RStudio Pro V1.1717-3 software, were used to compute the average yearly (soil loss, Sediment yield, and Tolerable Soil loss erosion) as follows.

### 4.1 $R_E$ factor

The rainfall in the Kanarwe River basin ranges from 700 mm to 950 m Table 5. Penjween is located within the watershed, while Chwarta-Mawat station is close to the basin's outlet; thus, these two stations significantly weigh $R_E$ factor estimation. A high $R_E$ -value (3011) is presented east, characterized by stormy weather and heavy intense rainfall. The western parts have a low $R_E$-value (1817), characterized by low terrain with less rainfall Figure 5.

Table 5- $R_E$ Factor Value.

| Stations | Rainfall (mm) | $RE$ [MJ mm $h^{-1}ha^{-1}year^{-1}$] |
|---|---|---|
| Penjween | 950 | 3011.74 |
| Chwarta-Mawat | 700 | 1838.88 |

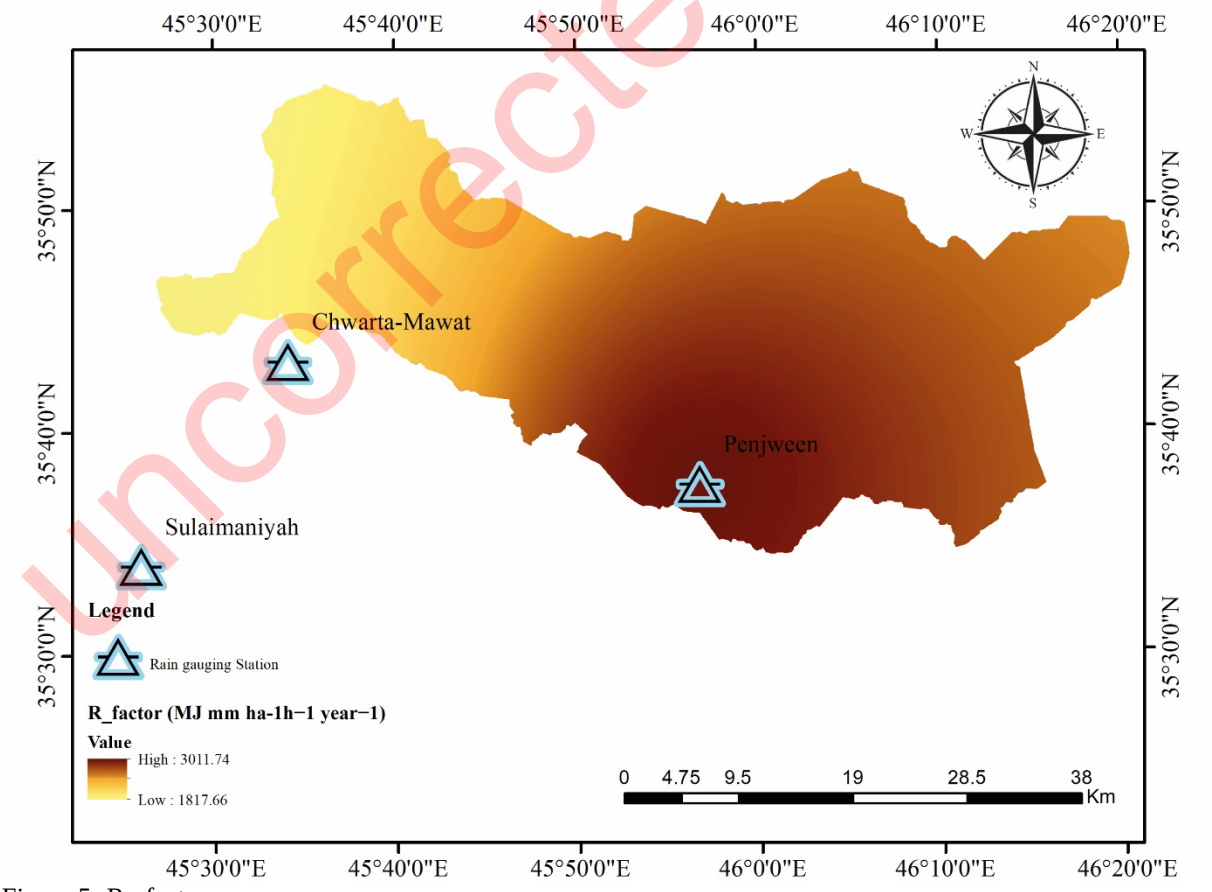


Figure 5- $R_E$ factor map.

### 4.2 $K_s$ factor

The Ks factor was computed based on four soil types: Lithosols, Chromic Vertosols, Calcic xerosols Lithosols, and Calcic Xerosols (Figure 5). The K values are estimated and compared to previous research on soil types in the northeastern part of Iraq (David, 1988; Hussein et al., 2007; Othman et al., 2021; Zakerinejad and Maerker, 2015). Accordingly, high $K_S$ values (0.065) are presented for chromic and clastic xeroslos in the west part and low values of $K_S$ (0.01, 0.04) in the east region Figure 6a and Figure 6b. This substantial variation in $K_S$ value is due to cropping out different rock types in the Kanarwe River basin.

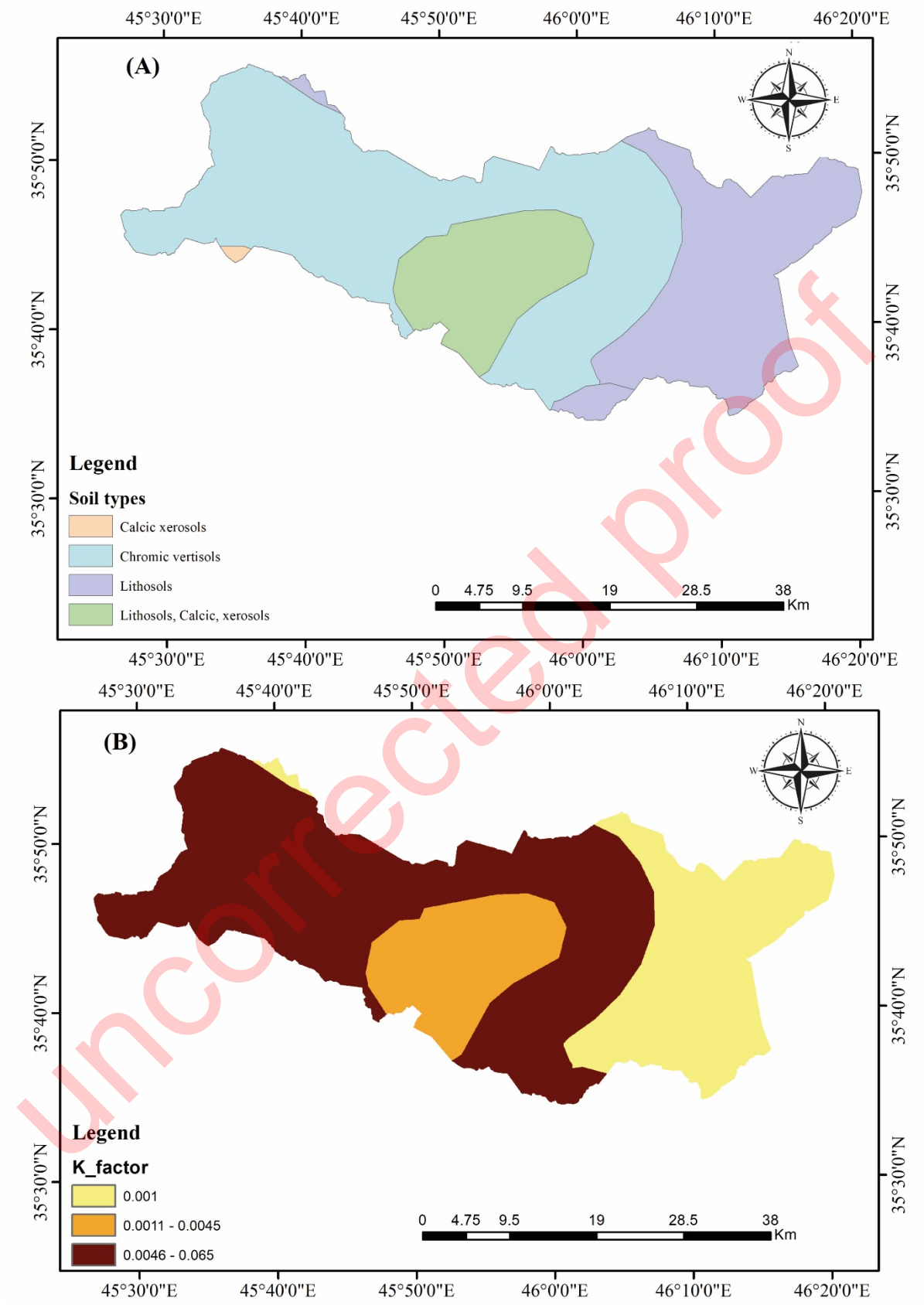


Figure 6- a) Soil map, b) $K_S$ factor map.

### 4.3 $LS_T$ factor

The maximum value of $LS_T$ is (26.6) when slope length and flow accumulation are high due to high altitude mountain and dense stream order in the watershed. The $LS_T$ values become lower closer to the river (flat areas) of the Siwil River in the lower regions Figure 7.

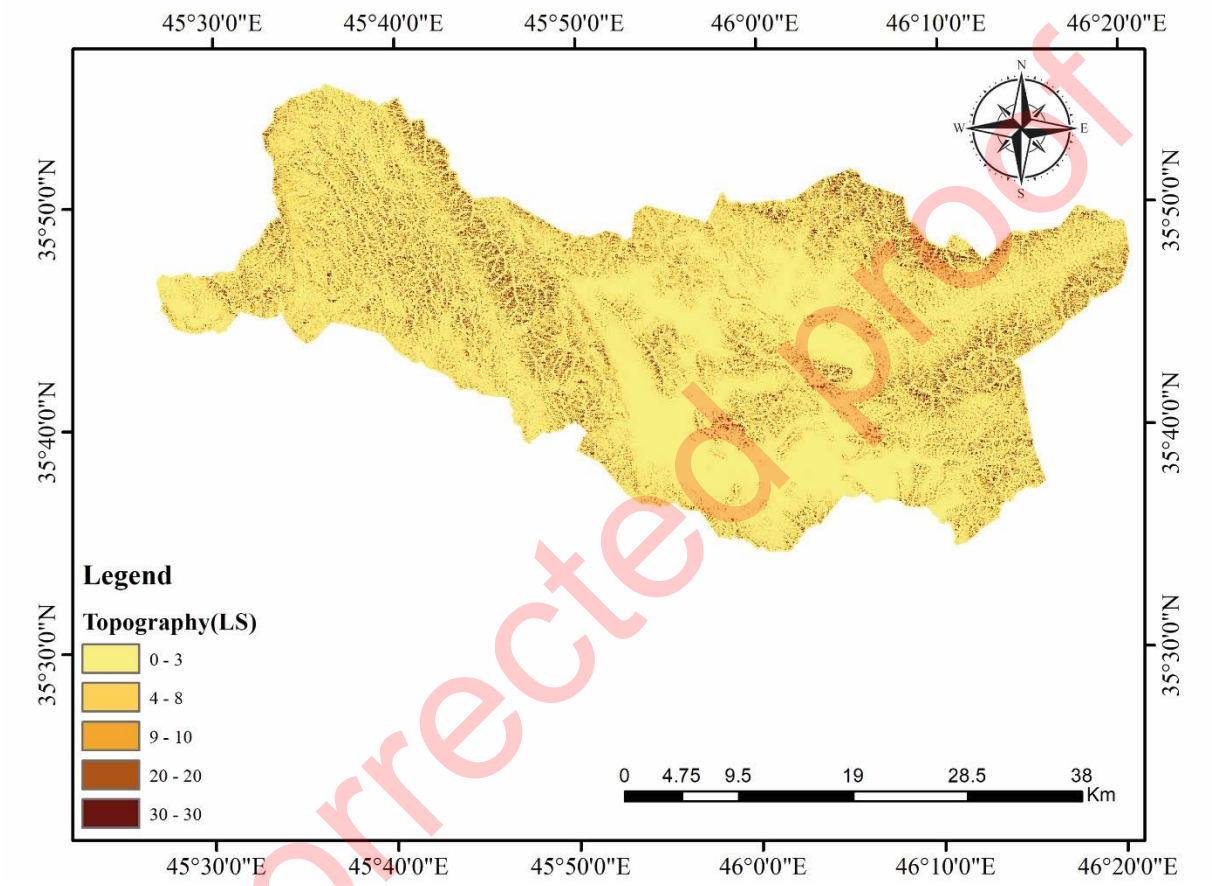


Figure 7- $LS_T$ factor map.

### 4.4 $P_S$ factor

The Kanarwe river basin was classified into five classes of Slope percentage (slope %) Figure 8a, and then the $P_S$-value was assigned for each type of slope percent Figure 8b based on Table 4. Most of the lower $P_S$-value is given to the central part, which is flatter and contains flood plains. The West of the Kanarwe River basin shows a high $P_S$-value due to the topographic condition.

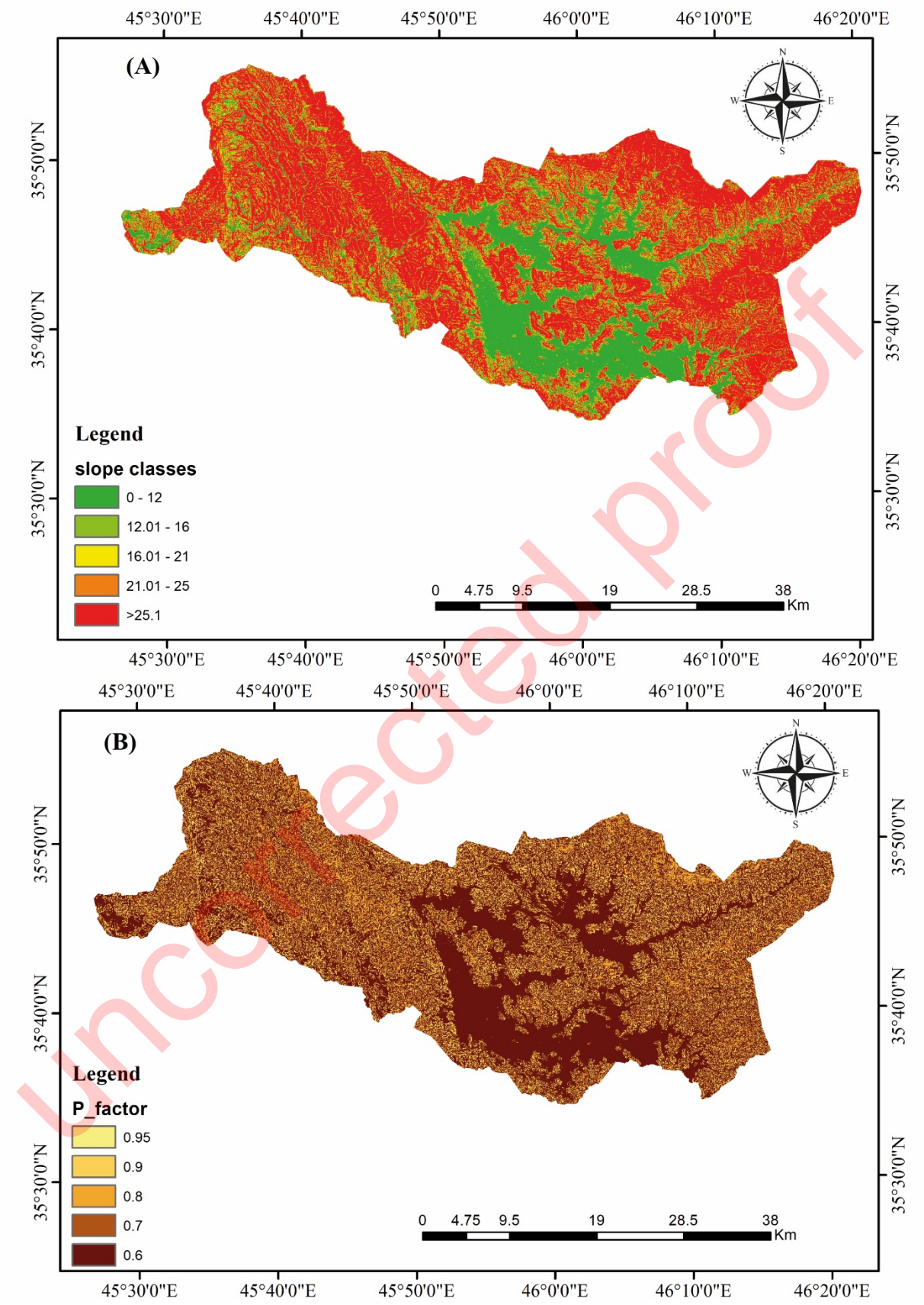




Figure 8- a) Slope class map, b) P factor map.

The mainland cover/use was (cropland, bare soil, and forests) Figure- 9a. The $C_V$ value ranges from (0.0012 to 0.37) and is assigned to land cover types of the Kanarwe river basin Figure 9b. Lower $C_V$ factor values (0.0012) were observed in the eastern and south-eastern parts due to the present forests, especially oak trees .The higher $C_V$ factor values (0.37) can be seen in the western parts, this area covers mostly weathered soils and recent deposits; hence it is more prone to water erosion.

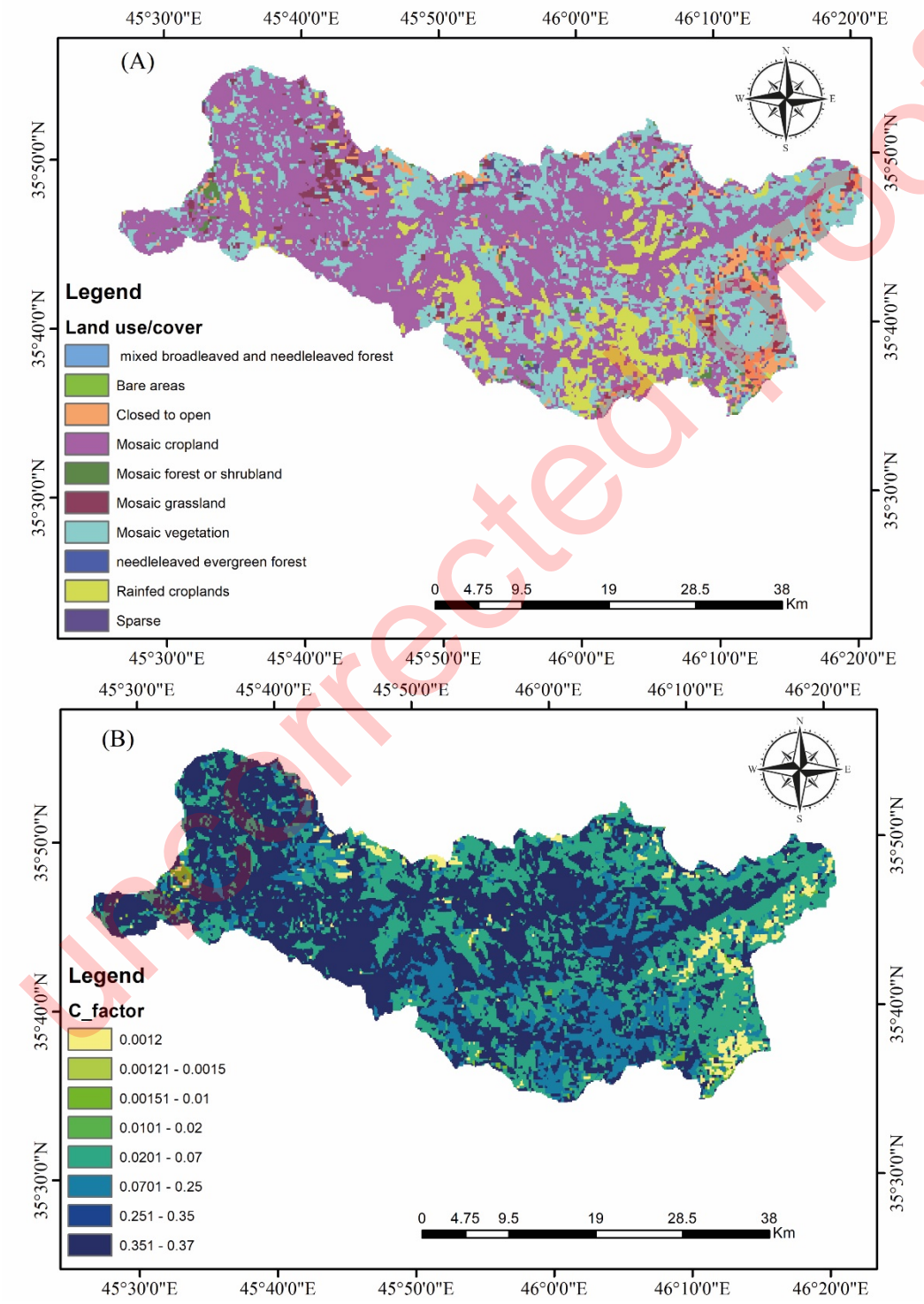


Figure 9- a) Land cover map, b) $C_v$ factor map.

**4.6 Soil loss and tolerance**

The final map of the soil loss was calculated using Equation 2 by integrating RUSLE layers (Parameters) to produce a grid map Figure 10. The soil loss rate expands from 0 in the east part (unweathered hard igneous) to 58.1 t $ha^{-1}$ $yr^{-1}$ in the central and west parts of the high weathered, sedimentary rock. The soil loss map was reclassed into five soil-lowering risk zones Table 6, using Gelagay and Minale, 2016 classification.

Table 6- Soil Loss class, covered area, and soil risk class.

| Soil loses | Soil erosion risk | Area (ha) | Percent of total area | Annual soil Loss(tone) | Percent of total soil loss |
|---|---|---|---|---|---|
| 0-7.0 | Low | 115575 | 74.4 | 404512 | 38.99 |
| 7.1-15 | Moderate | 22498.6 | 14.6 | 235200 | 22.67 |
| 15.1-25 | High | 10170.6 | 6.6 | 203412 | 19.6 |
| 25.1-45 | Very high | 4160.7 | 2.7 | 145624 | 14.03 |
| 45-60 | Sever | 924.6 | 0.6 | 48541 | 4.67 |

The calculation means annual soil loss is useless scientifically without the calculation of soil erosion risk classes (Pennock, 2019), so soil erosion risk was calculated and reclassed. The total annual soil loss is 1037289 t $ha^{-1}$ $yr^{-1}$; 404512, which covers 75% of the Kanarwe river basin, is below soil erosion risk (3.9 mm $yr^{-1}$) (Pennock, 2019). The FAO's (2019) tolerable soil loss rate is 4.2-7.2 t $ha^{-1}$ $yr^{-1}$ (Montgomery, 2007; Verheijen et al., 2009). Most of this low tolerable soil risk erosion is in the eastern and central parts due to the crop out of the un-weathered, hard rock of igneous rock and thin soil depth. The moderate to severe soil risk classes, which cover 25 % of the Kanarwe river basin, have an annual loss equal to 632777, above FAOs tolerable soil rate. This moderate to severe tolerable soil rate of the western and central part is spatially situated in the narrower, steep slope close to the outlet Figure 9.

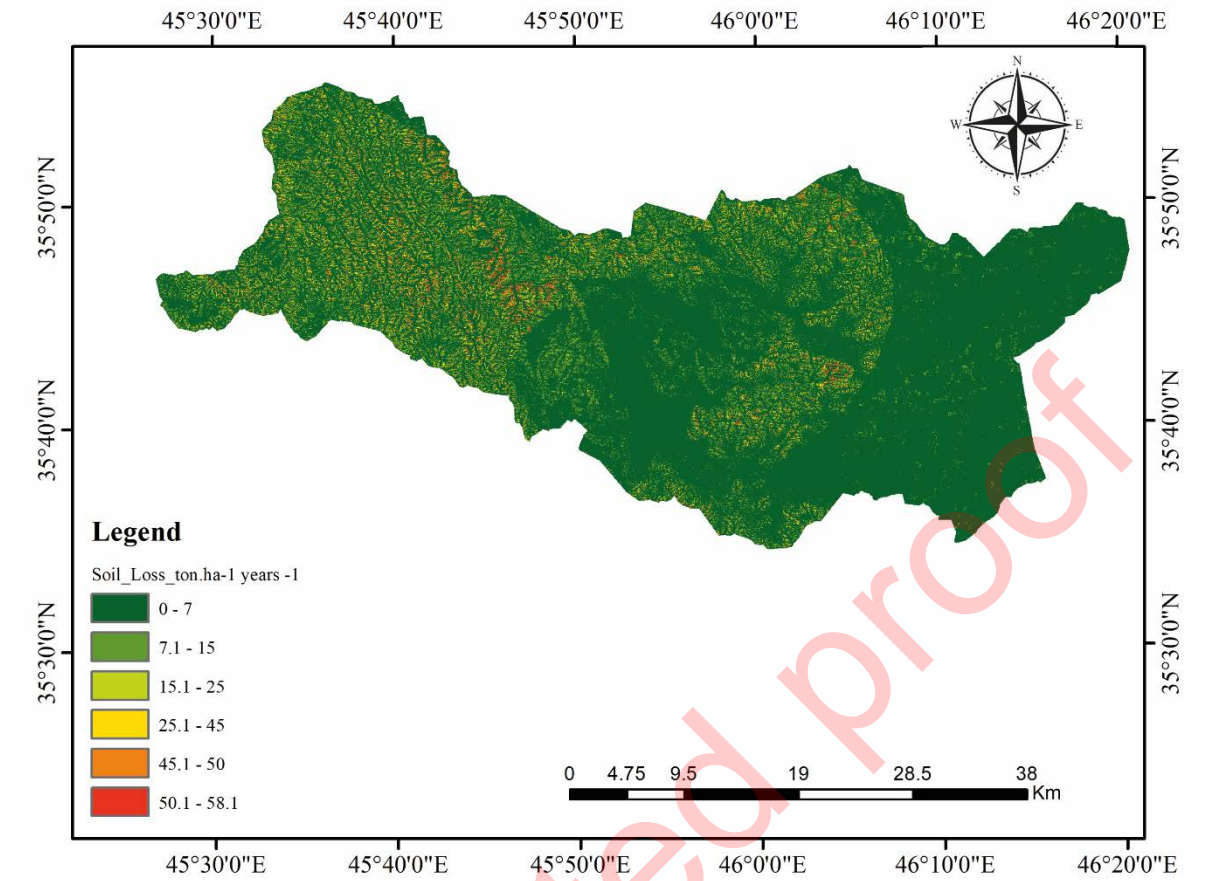


Figure 10- $S_{loss}$ map.



### 4.7 The sediment delivery ratio (SDR)

The SDR 0.5022 tons is calculated based on Equation 2 and Table 7. The drainage area and relief-length ratio are related to the time and rate of peak flow and the runoff. The SCS-CN parameter is more sensitive to the basin's soil types and land cover and calculates daily surface runoff ( USDA, 1986; Mishra et al., 2006; Kayet et al., 2018). the CN values for each land-use class are calculated and then listed in the supplementary material Table 8 and converted in Grid format Figure 11.

Table 7- Drainage Basin parameters.

| | | |
|---|---|---|
| Drainage area (DA) | 1543 $Km^2$ | ArcGIS 18.1 |
| Relief-length ratio (RL) | 3.122 | WMS 11.1 |

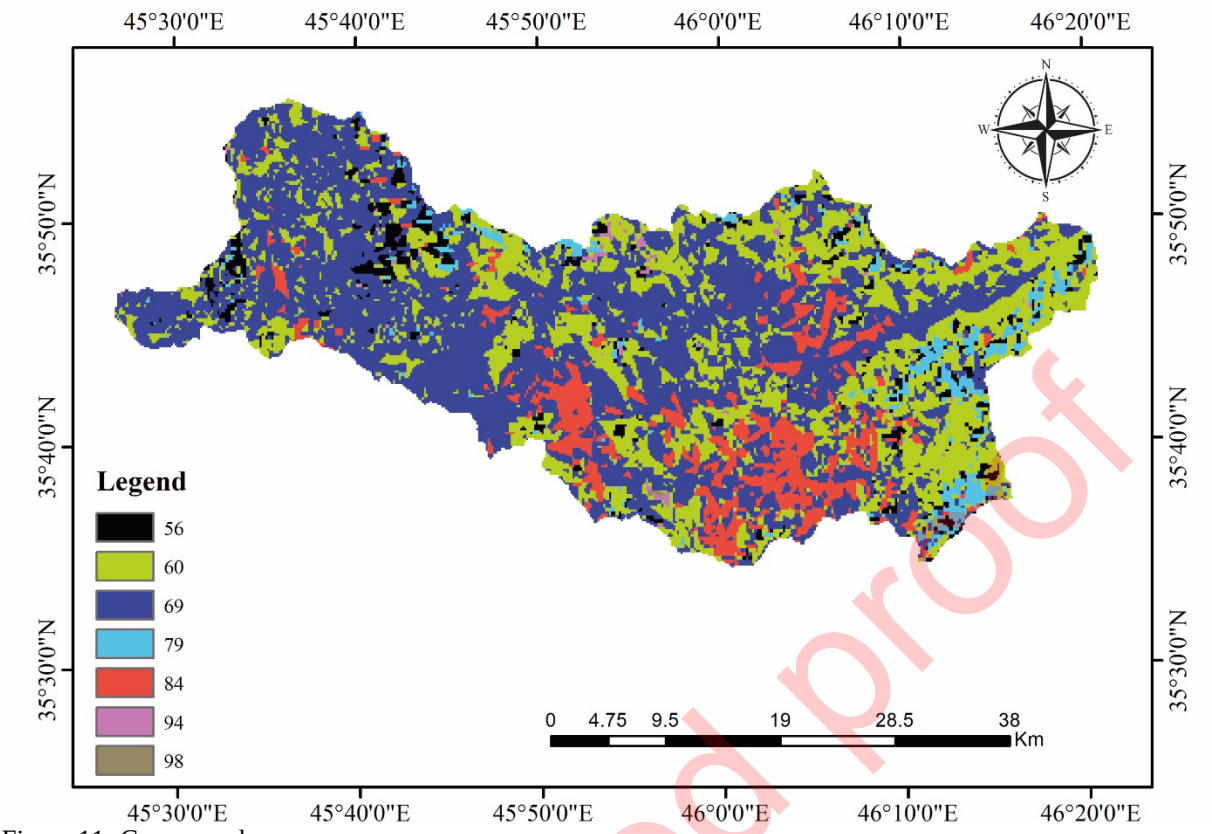


Figure 11- Curve number map.

Table 8- Runoff Curve Number values for each class of landcover types.

| HSG (Harmonized Soil Group) | Land Use Description | CN code | Area (km^2) | Product (CN x A) |
|---|---|---|---|---|
| D | Sparse (<15%) vegetation | 94 | 481.359 | 45247.74 |
| D | Closed to open (>15%) (broadleaved or needleless | 77 | 21.111 | 1625.541 |
| D | Rainfed croplands | 84 | 72.466 | 6087.131 |
| D | Mosaic vegetation (grassland/shrubland/forest) | 79 | 114.837 | 9072.155 |
| D | Mosaic forest or shrubland (50-70%) / grassland | 77 | 22.009 | 1694.713 |
| D | Mosaic cropland (50-70%) / vegetation (grassland | 84 | 123.072 | 10338.06 |
| D | Bare areas | 98 | 13.176 | 1291.21 |
| D | Mosaic grassland (50-70%) / forest or shrubland | 77 | 16.919 | 1302.738 |
| D | Closed (>40%) broadleaved deciduous forest (>5 | 79 | 1.946 | 153.765 |
| D | Closed (>40%) needle-leaved evergreen forest (> | 79 | 1.797 | 141.937 |
| B | Sparse (<15%) vegetation | 86 | 181.614 | 15618.79 |
| B | Mosaic vegetation (grassland/shrubland/forest) | 60 | 120.227 | 7213.646 |
| B | Mosaic grassland (50-70%) / forest or shrubland | 56 | 39.826 | 2230.271 |
| B | Mosaic cropland (50-70%) / vegetation (grassland | 69 | 105.105 | 7252.274 |
| B | Rainfed croplands | 69 | 155.562 | 10733.78 |
| B | Closed to open (>15%) (broadleaved or needleless | 56 | 22.758 | 1274.441 |
| B | Mosaic forest or shrubland (50-70%) / grassland | 56 | 37.131 | 2079.351 |

| | | | | |
|---|---|---|---|---|
| B | Bare areas | 98 | 12.277 | 1203.173 |
| D | Water bodies | 0 | 0.15 | 0 |
| B | Closed (>40%) broadleaved deciduous forest (>5 | 60 | 5.689 | 341.368 |
| CN | (Weighted) = Total Product \ Total Area | 80.6 | | |

### 3.8 The sediment yield (SY)

The sediment yield rate is calculated based on Equation 3. It is between 0 to 29.06 1 t. $ha^{-1}$ $yr^{-1}$ and the mean value is 0.321 Figure 12. The (Sy) becomes higher in the western part compared to the central areas and becomes lower in the east due to geological conditions dominated by hard un-weathered igneous rocks, the obtained results were well matched with the international soil erosion map of the world Global soil degradation map (Source: UNEP, International Soil Reference and Information Centre) and reveals soil degradation states in Iraq and Iran.

## 4. Correlation matrix between RUSLE variables and soil loss

The correlation coefficient analysis among RUSLE parameters shows that the $LS_T$, $K_s$, $C_v$, and $P_s$ factors showed a linear relationship with soil loss and sediment yield. In contrast, the R-factor showed an inverse relationship between sediment yield and soil loss Figure 13. The topography ($LS_T$) was more robust, influencing soil loss and sediment yield. A negative $R_E$ value reveals nature and climate conditions in the Kanarwe river basin. (Mohamadi and Kavian, 2015) Conclude that during periods of intense rainfall, the relation between the soil loss-rainfall fitted with nonlinear functions, because it's the beginning rainstorm until 30 minutes there no soil erosion later with prolonged rainfall the soil saturation crosses the limit of plasticity so as a result the weather layers start eroded the erosion decreases when this weathered layer is gone.

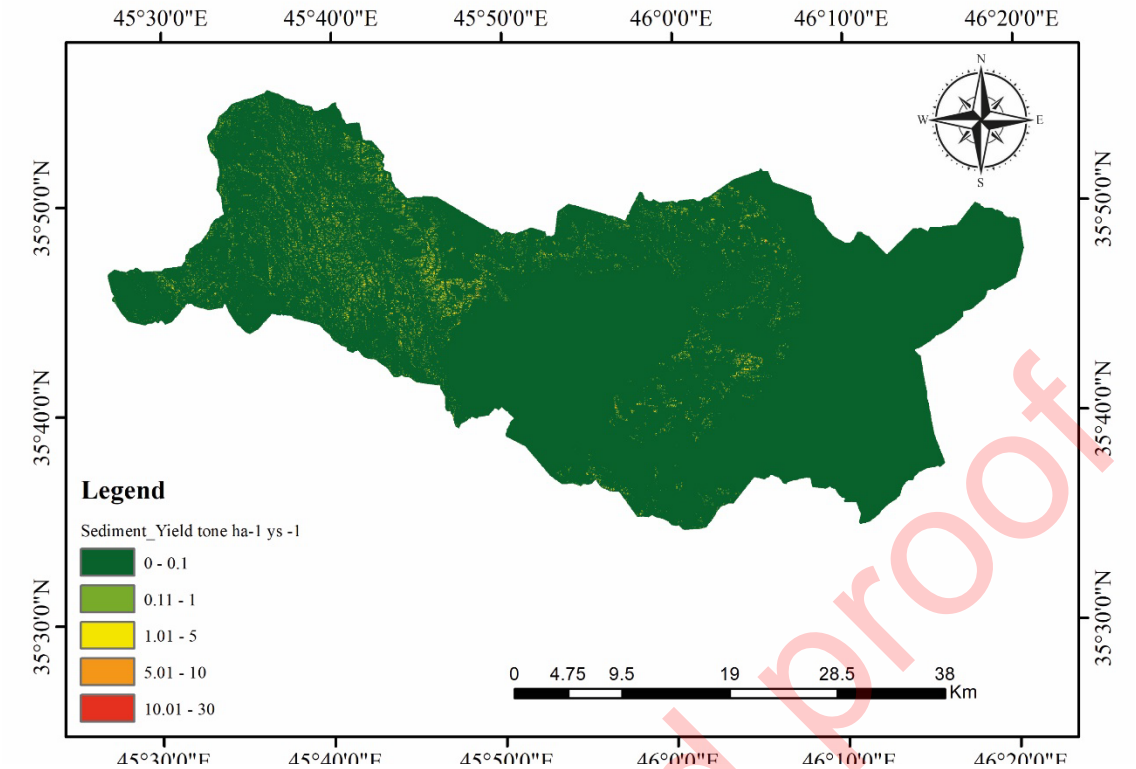


Figure 12- Sediment yield map.

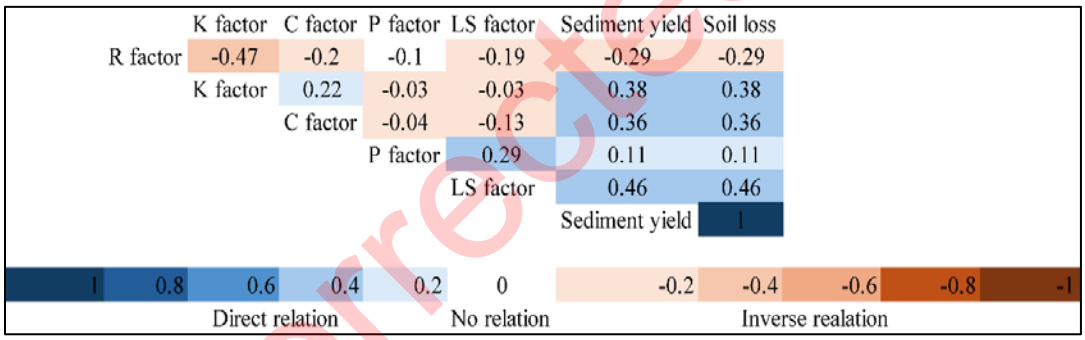


Figure 13- The correlation coefficient between RUSLE parameters.



## 5. Conclusion

Calculating soil loss, sediment yield, and soil erosion risk in a significant watershed like the Kanarwe river basin in Iraq by the RUSLE equation is very important. It guarantees the construction of any infrastructure, such as dams, railroads, urbanization, food production, and agriculture in the present and future. This study's findings include a spatially distributed mean annual soil loss, sediment yield, and tolerable soil loss in the Kanarwe river basin. The annual soil loss rate is extended from 0 to 58 t $ha^{-1}$ $yr^{-1,}$ while the sediment yield is between sediment 0 to 30 t $ha^{-1}$ $yr^{-1}$. About 25 % of the watershed is moderate to severe, above FAOs tolerable soil loss rate, and 75% is below FAOs tolerable soil loss, this result reveals that the soil condition is degradation condition in Iraq and Iran. However, the main factors controlling the soil loss are topography, soil erodibility, and crop factors instead of rainfall erosivity R factor due to the geological condition Kanarwe river basin. The statistical

analysis reveals that topography flysch rocks denudation makes the soil in ZSZ more vulnerable to weathering and erosion but less by anthropogenic factors. Finally, this study recommends the construction of sand dams in narrow gorges and artificial plantations at steep slopes upstream to control soil erosion risk effectively. The estimation of gully erosion is recommended because the RUSLE does not consider it.

**Acknowledgement**

The authors deeply thank Dr. Chiara Piccini and Dr. Karwan Mustaf (University of Charmo) for their fruitful discussions. Also, would like to Dr. katepina giam (University of California), and Dr Anwar O. Mohmmed (University of Sulaimani) for proofreading the manuscript and finally thank Mr Rebar Qaradagh for providing valuable information about the geology and soil condition of the study area.

**References**

Abbas, N., Wasimi, S. A., Al-Ansari, N. 2017. Impacts of climate change on water resources of Greater Zab and Lesser Zab Basins, Iraq, using soil and water assessment tool model. International Journal of Environmental, Chemical, Ecological, Geological and Geophysical Engineering 11, 823–829.

Alewell, C., Borrelli, P., Meusburger, K., Panagos, P. 2019. Using the USLE: Chances, challenges and limitations of soil erosion modelling. International Soil and Water Conservation Research 7, 203–225.

Al-Qayim, B. A., Baziany, M. M., Ameen, B. M. 2018. Mesozoic Tethyan Radiolarite age determination, Zagros suture zone, Kurdistan, NE Iraq. The Iraqi Geological Journal 17–33.

Anthony, E .J., Brunier, G., Besset, M., Goichot, M., Dussouillez, P., Nguyen, V. L. 2015. Linking rapid erosion of the Mekong River delta to human activities. Scientific reports 5, 1–12.

Ashiagbor, G., Forkuo, E. K., Laari, P., Aabeyir, R. 2013. Modeling soil erosion using RUSLE and GIS tools. Int J Remote Sens Geosci 2, 2013.

Balabathina, V. N., Raju, R. P., Mulualem, W., Tadele, G. 2020. Estimation of soil loss using remote sensing and GIS-based universal soil loss equation in northern catchment of Lake Tana Sub-basin, Upper Blue Nile Basin, Northwest Ethiopia. Environ Syst Res 9, 35.

Band, S. S., Chandra Pal, S., Bateni, S. M., Jun, C., Saha, A., Chowdhuri, I., Tiefenbacher, J. P., Janizadeh, S. 2022. Using computational-intelligence algorithms and remote sensing data to optimize the locations of check dams to control sediment and runoff in Kandolus watershed, Mazandaran, Iran. Geocarto International 1–23.

Benavidez, R., Jackson, B., Maxwell, D., Norton, K. 2018. A review of the (Revised) Universal Soil Loss Equation ((R) USLE): with a view to increasing its global applicability and improving soil loss estimates. Hydrol. Earth Syst. Sci 22, 6059–6086.

Bhattarai, R., Dutta, D. 2007. Estimation of Soil Erosion and Sediment Yield Using GIS at Catchment Scale. Water Resour Manage 21, 1635–1647.

Buringh, P., 1960. Soils and soil conditions in Iraq.

Chadli, K., 2016. Estimation of soil loss using RUSLE model for Sebou watershed (Morocco). Modeling Earth Systems and Environment 2, 1–10.

Chen, P., Feng, Z., Mannan, A., Chen, S., Ullah, T., 2019. Assessment of Soil Loss from Land Use/Land Cover Change and Disasters in the Longmen Shan Mountains, China. Appl. Ecol. Environ. Res 17, 11233–11247.

Chuenchum, P., Xu, M., Tang, W. 2020. Estimation of Soil Erosion and Sediment Yield in the Lancang–Mekong River Using the Modified Revised Universal Soil Loss Equation and GIS Techniques. Water 12, 135.

David, W. P. 1988. Soil and water conservation planning: policy issues and recommendations. Philippine Institute for Development Studies.

English, J. M., Lunn, G. A., Ferreira, L., Yacu, G. 2015. Geologic evolution of the Iraqi Zagros, and its influence on the distribution of hydrocarbons in the Kurdistan region. AAPG Bulletin 99, 231–272.

Ezz-Aldeen, M., Hassan, R., Ali, A., Al-Ansari, N., Knutsson, S. 2018. Watershed Sediment and Its Effect on Storage Capacity: Case Study of Dokan Dam Reservoir. Water 10, 858.

Ezzaouini, M. A., Mahé, G., Kacimi, I., Zerouali, A. 2020. Comparison of the MUSLE Model and Two Years of Solid Transport Measurement, in the Bouregreg Basin, and Impact on the Sedimentation in the Sidi Mohamed Ben Abdellah Reservoir, Morocco. Water 12, 1882.
Gashaw, T., Tulu, T., Argaw, M., Worqlul, A.W. 2017. Evaluation and prediction of land use/land cover changes in the Andassa watershed, Blue Nile Basin, Ethiopia. Environ Syst Res 6, 17.
Gelagay, H.S., Minale, A.S., 2016. Soil loss estimation using GIS and Remote sensing techniques: A case of Koga watershed, Northwestern Ethiopia. International Soil and Water Conservation Research 4, 126–136.
Gholami, L., Khaledi Darvishan, A., Spalevic, V., Cerdà, A., Kavian, A. 2021. Effect of storm pattern on soil erosion in damaged rangeland; field rainfall simulation approach. J. Mt. Sci. 18, 706–715.
Hassan, R., Al-Ansari, N., Ali, S.S., Ali, A.A., Abdullah, T., Knutsson, S. 2016. Dukan dam reservoir bed sediment, Kurdistan Region, Iraq. Engineering 8, 582–596.
Hosseinalizadeh, M., Alinejad, M., Mohammadian Behbahani, A., Khormali, F., Kariminejad, N., Pourghasemi, H. R., 2020. A Review on the Gully Erosion and Land Degradation in Iran, in: Shit, P.K., Pourghasemi, H.R., Bhunia, G.S. (Eds.), Gully Erosion Studies from India and Surrounding Regions, Advances in Science, Technology & Innovation. Springer International Publishing, Cham, 393–403.
Hussein, M. H., Kariem, T. H., Othman, A. K. 2007. Predicting soil erodibility in northern Iraq using natural runoff plot data. Soil and Tillage Research 94, 220–228. https://doi.org/10.1016/j.still.2006.07.012
Kayet, N., Pathak, K., Chakrabarty, A., Sahoo, S. 2018. Evaluation of soil loss estimation using the RUSLE model and SCS-CN method in hillslope mining areas. International Soil and Water Conservation Research 6, 31–42.
Kebede, Y. S., Endalamaw, N. T., Sinshaw, B. G., Atinkut, H. B. 2021. Modeling soil erosion using RUSLE and GIS at watershed level in the upper beles, Ethiopia. Environmental Challenges 2, 100009.
Lee, M., Yu, I., Necesito, I. V., Kim, H., Jeong, S. 2014. Estimation of sediment yield using total sediment yield formulas and RUSLE. Journal of the Korean Society of Hazard Mitigation 14, 279–288.
Ma'ala, K. A. 2007. The Geology of Sulaimaniya Quadrangle Ni-38-3 (Ghm-10) Scale 1: 250 000.
Mishra, S. K., Tyagi, J. V., Singh, V. P., Singh, R. 2006. SCS-CN-based modeling of sediment yield. Journal of Hydrology 324, 301–322.
Mohamadi, M. A., Kavian, A. 2015. Effects of rainfall patterns on runoff and soil erosion in field plots. International soil and water conservation research 3, 273–281.
Mohammad, F. O. 2023. Engineering geological assessment of proposed goma-qazan dam site within Kanarwe rive sub basin and its hydrological conditions Sulaymaniyah-NE Iraq. Unpublished.
Mohammed, F., Al-Manmi, D.A., Al-Manmi, A., Hamasur, G. 2023. The Efficiency of SCS-CN, HEC-1, HEC-HMS, TR55, RATIONAL, and SNYDER UNIT Hydrograph Models for Determining Peak Flood Discharge in the Upper Part of Lesser Zab Basin, Kurdistan Region, Iraq. IRAQI BULLETIN OF GEOLOGY AND MINING 19, 163–179.
Mohammed, F. O., Mohammad, A. O., Ibrahim, H. S., Hasan, R. A. 2021. Future Scenario of Global Climate Map change according to the Köppen-Geiger Climate Classification. Baghdad Science Journal 18, 1030–1030.
Montgomery, D. R. 2007. Soil erosion and agricultural sustainability. Proceedings of the National Academy of Sciences 104, 13268–13272.
Nachtergaele, F. O., van Velthuizen, H., Verelst, L., Batjes, N. H., Dijkshoorn, J. A., van Engelen, V. W. P., Fischer, G., Jones, A., Montanarella, L., Petri, M. 2008. Harmonized world soil database (version 1.0).
Omeed H. Al-Kakey, Arsalan A. Othman, Broder J. Merkel. 2022. Kuwait Journal of Science 50, 19.
Ostovari, Y., Moosavi, A. A., Mozaffari, H., Poppiel, R. R., Tayebi, M., Demattê, J. A. 2022. Soil erodibility and its influential factors in the Middle East, in: Computers in Earth and Environmental Sciences. Elsevier, pp. 441–454.
Othman, A. A., Obaid, A. K., Al-Manmi, D. A. M. A., Al-Maamar, A. F., Hasan, S. E., Liesenberg, V., Shihab, A. T., Al-Saady, Y. I. 2021. New Insight on Soil Loss Estimation in the Northwestern Region of the Zagros Fold and Thrust Belt. ISPRS International Journal of Geo-Information 10, 59.
Othman, A. A., Obaid, A. K., Sissakian, V. K., Maamar, A. F. A., Shihab, A. T. 2022. RUSLE Model in the Northwest Part of the Zagros Mountain Belt, in: Environmental Degradation in Asia. Springer, 287–306.
Pennock, D. J. 2019. Soil erosion: The greatest challenge for sustainable soil management. Food and Agriculture Organization of the United Nations.
Pimentel, D., Burgess, M. 2013. Soil erosion threatens food production. Agriculture 3, 443–463.
Renard, K. G. 1997. Predicting soil erosion by water: a guide to conservation planning with the Revised Universal Soil Loss Equation (RUSLE). United States Government Printing.
Renard, K. G., Freimund, J. R. 1994. Using monthly precipitation data to estimate the R-factor in the revised USLE. Journal of Hydrology 157, 287–306. https://doi.org/10.1016/0022-1694(94)90110-4
Sadeghi, S. H. R. 2017. Soil erosion in Iran: state of the art, tendency and solutions. Poljoprivreda i Sumarstvo 63, 33–37.

Salar, S. G. 2022. Water and sediments yields estimation: A case study in Bawashaswar Watershed/Iraqi Kurdistan Region. Kuwait Journal of Science 49.
Shin, G. J. 1999. The analysis of soil erosion analysis in watershed using GIS. Department of Civil Engineering, Gang-won National University, Gangwon-do, South Korea, Ph. D. dissertation.
Shubbar, R. M., Salman, H. H., Lee, D.-I. 2017. Characteristics of climate variation indices in Iraq using a statistical factor analysis. International Journal of Climatology 37, 918–927.
Simms, A. D., Woodroffe, C. D., Jones, B. G. 2003. Application of RUSLE for erosion management in a coastal catchment, southern NSW.
Somasiri, I., Hewawasam, T., Rambukkange, M. 2021. Adaptation of the revised universal soil loss equation to map spatial distribution of soil erosion in tropical watersheds: a GIS/RS-based study of the Upper Mahaweli River Catchment of Sri Lanka. Modeling Earth Systems and Environment 1–19.
Tiwary, P., Patil, N., Bhattacharyya, T., Chandran, P., Ray, S., Karthikeyan, K., Sarkar, D., Pal, D., Prasad, J., Mandal, C. 2014. Pedotransfer functions: a tool for estimating hydraulic properties of two major soil types of India. Current Science 1431–1439.
USDA, S. 1986. Urban hydrology for small watersheds. Technical release 55, 2–6.
Verheijen, F. G., Jones, R. J., Rickson, R., Smith, C. 2009. Tolerable versus actual soil erosion rates in Europe. Earth-Science Reviews 94, 23–38.
Wischmeier, W. H., Smith, D. D. 1978. Predicting rainfall erosion losses: a guide to conservation planning. Department of Agriculture, Science and Education Administration.
Yang, D., Kanae, S., Oki, T., Koike, T., Musiake, K. 2003. Global potential soil erosion with reference to land use and climate changes. Hydrological processes 17, 2913–2928.
Zakerinejad, R., Maerker, M. 2015. An integrated assessment of soil erosion dynamics with special emphasis on gully erosion in the Mazayjan basin, southwestern Iran. Natural Hazards 79, 25–50.
Zare, M., Mohammady, M., Pradhan, B. 2017. Modeling the effect of land use and climate change scenarios on future soil loss rate in Kasilian watershed of northern Iran. Environmental Earth Sciences 76, 1–15.